Control of a nonholonomic mobile robot via sensor-based target tracking and pose estimation

M. Maya-Mendez, P. Morin, C. Samson
INRIA Sophia-Antipolis – ICARE Team
2004 Route des Lucioles, BP 93
06902 Sophia-Antipolis Cedex, France
{Mauro.Maya_Mendez,Pascal.Morin,Claude.Samson}@inria.fr

***Abstract*— The paper addresses the problem of controlling the posture of a nonholonomic mobile robot via sensor-based target tracking. The control technique here considered is adapted from the Transverse Function approach with sensory signals used to calculate an estimate of the relative pose of the robot with respect to the target. An analysis of stability and robustness w.r.t. pose estimation errors is presented and the overall control performance is tested via simulation and experimentation on a unicycle-type mobile robot equipped with a camera.**

I. Introduction

Sensor-based control, which consists essentially in using exteroceptive measurements in feedback loops, is an important technique for robotic applications that require the positioning of the controlled robotic device with respect to (w.r.t.) some external object/target. It has first been developped for, and applied to, manipulator arms [1]–[4] in order to perform tasks such as pick and place, welding, or pointing, by using the information about the surrounding environment provided by exteroceptive sensors. Many sensor-based applications have also emerged from the more recent development of mobile robotics. For example, visual servoing is used for path following, target tracking, or platooning tasks [5], [6]. The present study is devoted to the sensor-based control of nonholonomic mobile robots with a focus on robotic tasks which rely on the monitoring of *both* the position and orientation of the robot, i.e. on the control of the complete posture of the mobile platform. An abundant literature has been devoted to the control of nonholonomic systems in order to tackle various challenging issues associated with the problem. Two of the authors of the present paper have worked on these questions for years and the reader is referred to [7] where these issues are surveyed is some detail. Among them, the problem of stabilizing state trajectories which are not necessarily feasible for the system has received little attention, whereas we believe that it is very relevant for a number of applications, an example of which is treated further. The fact that non-feasible trajectories cannot, by definition, be asymptotically stabilized, combined with other difficulties and impossibilities (see [7] and [8], for instance) related to Brockett's theorem [9] according to which asymptotic stabilization of a fixed point is not solvable by using smooth pure-state feedback, and also the common experience that infinite precision in the posture monitoring of a mobile robot is seldom necessary in practice, suggests that, for nonholonomic systems, the classical objective of *asymptotic* stabilization of a desired (reference) state or trajectory is not best suited to qualify what can be achieved with feedback control. By contrast, the slightly weaker objective, considered in [10], of asymptotic stabilization of a set contained in an arbitrarily small neighborhood of the reference state allows to avoid all theoretical obstructions associated with the former objective. Its satisfaction guarantees, for instance, that the tracking error can be ultimately bounded by a pre-specified (non-zero) value, whether the reference trajectory is, or is not, feasible (provided only that it is smooth enough). The Transverse Function (TF) approach, the basics of which are described in [10], provides a way of designing smooth feedback laws which satisfy this objective. Experimental validations of this approach for the tracking of an omnidirectional target have been reported in [11], [12]. The present paper goes in the same direction, with the complementary preoccupation of studying the robustness of the control when the target is observed with sensors whose characteristics are either imperfectly modelled or purposefully simplified. With respect to the standard classification of sensor-based control methods (see e.g. [4]), the strategy considered here relies on pose estimation. The main contribution of the paper is the derivation of sufficient conditions upon the pose estimation method under which closed-loop stability is granted. In particular, we prove that a crude pose estimation obtained by using an estimate of the sensor's interaction matrix can yield good tracking precision. This analysis is illustrated and complemented by simulation and experimental results. For simplicity, the exposition is restricted to unicycle-type mobile robots. However, it can readily be extended to other platforms –car-like vehicles, in particular– due to the generality of the TF approach.

The paper is organized as follows. The studied control problem is presented in Section II. Kynematic models and basic results about the application of the TF approach to the design of practical stabilizers are recalled in Section III. Combining sensor-based pose estimation and control is addressed in Section IV, along with stability conditions for the resulting sensor-based controllers. Due to space limitations, the proofs of the stability results are omitted (they are available upon request to the authors). The control approach is then validated, first via simulation results in Section V, then via experimental results in Section VI.

II. PROBLEM STATEMENT

Consider the setup depicted on Fig. 1. The unicycle-like

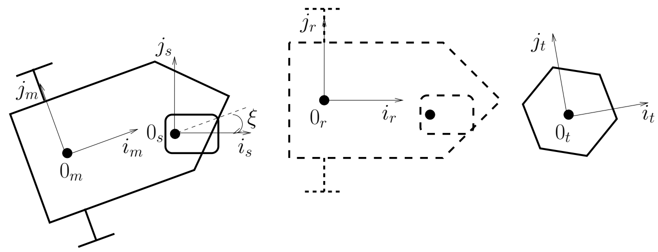

Fig. 1. Mobile robot (l), reference situation (m), and target (r)

robot (on the left-side) is equipped with a sensor (a camera, for instance) providing information about its relative situation w.r.t. a moving object, called the *target*. For simplicity, all bodies are represented by their projections on the robot's plane of motion. A frame $\mathcal{F}_m = \{0_m, \overrightarrow{\imath_m}, \overrightarrow{\jmath_m}\}$ is attached to the mobile platform, and g_{om} denotes the situation of this frame w.r.t. some fixed frame $\mathcal{F}_0$. This is an element of the Special Euclidean group $SE(2)$, itself isomorphic to $\mathbb{R}^2 \times \mathbb{S}^1$. Another frame $\mathcal{F}_s = \{0_s, \overrightarrow{\imath_s}, \overrightarrow{\jmath_s}\}$ is attached to the sensor, and g_{os} denotes the situation of this frame w.r.t. $\mathcal{F}_0$. The relative situation g_{ms} of the sensor w.r.t. the platform is parameterized by the pan angle ξ which is measured and whose control can be performed on the basis of the simple kynematic model $\dot{\xi} = v_\xi$, with v_ξ the associated velocity control variable. The sensor delivers a vector-valued signal $s \in \mathbb{R}^3$ which only depends on the relative situation g_{ts} of the sensor frame w.r.t. a frame $\mathcal{F}_t = \{0_t, \overrightarrow{\imath_t}, \overrightarrow{\jmath_t}\}$ attached to the target, i.e. $s = \varphi(g_{ts})$. It is assumed that g_{ts} is uniquely defined by s, at least within some operating domain. In fact, we will make the stronger assumption that φ is a diffeomorphism from an open domain of $SE(2)$ to an open domain of $\mathbb{R}^3$. The control objective is to stabilize the platform at a reference situation, depicted in the middle of the figure, with the relative situation g_{tr} being predefined and constant. This is clearly equivalent to stabilizing at zero the relative situation $g = g_{rm}$ between the frames $\mathcal{F}_m$ and $\mathcal{F}_r$. Note that maintaining this "tracking error" at zero permanently is obviously not possible in all cases, due to the nonholomic constraint on the robot which forbids any instantaneous lateral motion. In fact, there are not many motions of the target for which this is possible. This is one of the reasons why practical stabilization, allowing for small tracking errors, is here preferred to the non-attainable classical objective of asymptotic stabilization which requires convergence of the error to zero.

III. MODELING AND PRELIMINARY RECALLS

A. *Group operation in $SE(2)$ and parametrization*

Since $SE(2)$ is a Lie group isomorphic to $\mathbb{R}^2 \times \mathbb{S}^1$, one can identify an element g of this group with a three-dimensional "vector" $(p', \theta)'$, with $p = (x, y)' \in \mathbb{R}^2$, $\theta \in \mathbb{S}^1$, and the prime superscript denoting the transpose operation. When using an element of this group, say $g_{om} = (p'_{om}, \theta_{om})'$, to characterize the situation of a frame, $\mathcal{F}_m$, with respect to another, $\mathcal{F}_o$, the vector p_{om} is the vector of coordinates of O_m in the frame $\mathcal{F}_o$ and θ_{om} is the oriented angle between $\overrightarrow{\imath_o}$ and $\overrightarrow{\imath_m}$.
$SE(2)$ is endowed with the group operation defined by

$$(g_1, g_2) \longmapsto g_1 g_2 := \begin{pmatrix} p_1 + R(\theta_1) p_2 \\ \theta_1 + \theta_2 \end{pmatrix} \quad (1)$$

with $R(\theta)$ the rotation matrix of angle θ. The unit element e of this group (such that $ge = eg = g$) is $e = (0, 0)$ and the inverse g^{-1} of g (such that $gg^{-1} = g^{-1}g = e$) is

$$g^{-1} = \begin{pmatrix} -R(-\theta)p \\ -\theta \end{pmatrix} \quad (2)$$

From now on, e will also be denoted as 0. It follows from these relations that the situation g_{ab} of a frame $\mathcal{F}_b$ w.r.t. a frame $\mathcal{F}_a$ satisfies the relation $g_{ab} = g_{oa}^{-1} g_{ob}$. Note also that $g_{ab} = g_{ba}^{-1}$ and $g_{ab} g_{ba} = 0$.
A distance between $g = (p', \theta)'$ and 0 is given[1] by $\|g\| = \sqrt{\|p\|^2 + \theta^2}$ with $\|p\|$ the Euclidean norm of the vector p, and θ identified with its representative in $(-\pi/2; \pi/2]$. Finally, we denote by $\mathrm{B_g}(\delta)$ the "ball" in $SE(2)$ of radius δ and centered at 0, i.e. $\mathrm{B_g}(\delta) = \{g \in SE(2) : \|g\| \leqslant \delta\}$.

B. *Kynematic models*

With $g_{om} = ((x_{om}, y_{om})', \theta_{om})'$ denoting the situation of the robot's frame $\mathcal{F}_m$ w.r.t. the fixed (inertial) frame $\mathcal{F}_o$, the well known kynematic equations of a unicycle-type mobile robot are:

$$\begin{cases} \dot{x}_{om} &= v_1 \cos\theta \\ \dot{y}_{om} &= v_1 \sin\theta \\ \dot{\theta}_{om} &= v_2 \end{cases} \quad (3)$$

or, in a more compact form:

$$\dot{g}_{om} = X(g_{om}) C v \quad (4)$$

with $v = (v_1, v_2)'$, v_1 and v_2 denoting the longitudinal and angular velocities of the mobile robot,

$$X(g) = \begin{pmatrix} \cos\theta & -\sin\theta & 0 \\ \sin\theta & \cos\theta & 0 \\ 0 & 0 & 1 \end{pmatrix}, \quad C = \begin{pmatrix} 1 & 0 \\ 0 & 0 \\ 0 & 1 \end{pmatrix} \quad (5)$$

The generalization of the above model to the situation $g := g_{rm}$ between the robot's frame and a *moving* reference frame with velocity vector $c_r(t)$ at time t, i.e. such that $\dot{g}_{or}(t) = X(g_{or}) c_r(t)$, is:

$$\dot{g} = X(g) \left(Cv - \mathrm{Ad}^X(g^{-1}) c_r(t) \right) \quad (6)$$

with

$$\mathrm{Ad}^X(g) = \begin{pmatrix} R(\theta) & \begin{pmatrix} y \\ -x \end{pmatrix} \\ 0 & 1 \end{pmatrix} \quad (7)$$

the matrix associated with the group adjoint operator.
Important: From now on, to simplify the notation, g will always stand for g_{rm}.

[1]with a slight abuse of notation because $SE(2)$ is not a vector space and thus cannot be endowed with a norm

The relative situation g can be viewed as a "tracking error" that the control v is in charge of stabilizing at zero. Relation (6) points out that it is not possible to keep this error equal to zero when the reference trajectory is not feasible for the nonholonomic platform, i.e. when the second component of $c_r(t)$ is different from zero. We recall in the next section the design of *practical* stabilizers based on the TF approach.

C. Practical stabilization based on the TF approach

The Transverse Function approach provides a general framework for the practical stabilization of nonholonomic systems. We recall hereafter some aspects of this approach applied to the unicycle, and refer the reader to [10] for more details.

Definition III.1 *A smooth function $f : \mathbb{T}^p \to SE(2)$, with $\mathbb{T}^p$ the p-dimensional torus (i.e. $\mathbb{T} = \mathbb{S}^1$) is called a* transverse function *for System* (4) *if, for any $\alpha \in \mathbb{T}^p$, the matrix*

$$\begin{pmatrix} X(f(\alpha))C & \frac{\partial f}{\partial \alpha}(\alpha) \end{pmatrix} \tag{8}$$

is of rank three $(= \dim(SE(2)))$.

Remark III.1 *Since $X(g)$ is an invertible matrix for any g, there exists a matrix $A(\alpha)$ such that $\frac{\partial f}{\partial \alpha}(\alpha) = X(f(\alpha))A(\alpha)$. Then, the matrix* (8) *is of rank three if and only if the matrix*

$$\bar{C}(\alpha) = (C \quad -A(\alpha)) \tag{9}$$

is also of rank three.

Example: One easily verifies that the function $f = (f_x, f_y, f_\theta)' : \mathbb{T}^1 \to SE(2)$ defined by

$$f(\alpha) \quad = \quad \begin{pmatrix} \varepsilon \sin \alpha \\ \frac{\varepsilon^2}{4}\eta \sin 2\alpha \\ \arctan(\varepsilon\eta\cos\alpha) \end{pmatrix} \tag{10}$$

is a transverse function for any $\varepsilon, \eta > 0$.

The following result shows that the knowledge of a transverse function allows to design feedback laws that guarantee *a)* the convergence of the tracking error g to a neighborhood of the origin, and *b)* the convergence of g to a fixed value when $c_r = 0$ (i.e. when the reference trajectory is fixed).

Proposition III.1 *Let f denote a transverse function for System* (4)*, and let $z = gf(\alpha)^{-1}$. Then,*
i) Along the solutions of the tracking error model (6)*, and for any smooth curve $\alpha(.)$,*

$$\dot{z} = X(z)\text{Ad}^X(f(\alpha))\left(\bar{C}(\alpha)\bar{v} - \text{Ad}^X(g^{-1})c_r(t)\right) \tag{11}$$

with $\bar{v} = (v', \dot{\alpha}')'$ and $\bar{C}(\alpha)$ defined by (9)*.*
ii) The matrix $\bar{C}(\alpha)$ being of rank three for any α, the change of variable

$$\bar{v} = \bar{C}(\alpha)^\dagger \left(\text{Ad}^X(f(\alpha)^{-1})v_z + \text{Ad}^X(g^{-1})c_r(t)\right) \tag{12}$$

with $\bar{C}(\alpha)^\dagger$ a right-inverse of $\bar{C}(\alpha)$, transforms System (11) *into $\dot{z} = X(z)v_z$.*
iii) For any Hurwitz-stable matrix K, and for v_z defined by

$$v_z = X(z)^{-1}Kz \tag{13}$$

- *a)* *$\|g\|$ is ultimately bounded by $\varepsilon_f := \max_\alpha \|f(\alpha)\|$ for* any *reference trajectory $g_r(.)$,*
- *b)* *if $c_r = 0$, g and g_{om} exponentially tend to fixed points in $SE(2)$.*

Property *iii.a)* is easily deduced from the (exponential) convergence of z to zero. Property *iii.b)* also follows from this convergence property. Indeed, when $c_r = 0$, $\bar{v}$ tends to zero exponentially, so that g, and g_{om} are bound to converge to fixed values.

Note that, with this approach, the derivative $\dot{\alpha}$ of the vector of variables (reduced to a scalar variable in the case of the example (10)) on which the transverse function depends plays the role of a complementary control vector.

IV. COMBINED POSE ESTIMATION AND CONTROL

In order to implement the control (12)-(13) in Prop. III.1, g has to be known at each time. In practice however, this information is often only available via the measurement provided by exteroceptive sensors embarked on the robot. Moreover, it is not completely accurate due to well known reasons such as imperfect modelling and calibration of the sensors. We now examine how the replacement, in the control expression, of g by a *pose estimate* $\hat{g}$ calculated from the sensory signal s modifies the above result.

A. Some techniques for pose estimation

Let us first recall that $s = \varphi(g_{ts})$ and that we have assumed that φ is a (local) diffeomorphism, so that φ^{-1} is also well defined locally. By the group law, one has $g = g_{rt}g_{ts}g_{sm}$, so that one can also write

$$g = g_{rt}\varphi^{-1}(s)g_{sm} \tag{14}$$

The calculation of an estimate $\hat{g}$ of g from sensory measurements corresponds to the classical "pose estimation problem", which has been widely studied in the robotics literature. Let us (without any claim of originality) briefly recall a few possible approaches. Pose estimation methods are usually termed as *model-based* or *model-free*, depending on the amount of information about φ that is needed to calculate $\hat{g}$. For example, it follows from (14) that $s = \varphi_s(g, \xi) := \varphi(g_{tr}gg_{ms})$. If s^* and ξ^* denote some values associated with the reference situation, i.e. $s^* = \varphi_s(0, \xi^*)$, then a model-free estimate can be obtained from the local approximation $s - s^* \approx \frac{\partial \varphi_s}{\partial g}(0, \xi^*)g + \frac{\partial \varphi_s}{\partial \xi}(0, \xi^*)(\xi - \xi^*)$, i.e.

$$\hat{g} = \left(\widehat{\frac{\partial \varphi_s}{\partial g}}(0, \xi^*)\right)^{-1}\left(s - s^* - \widehat{\frac{\partial \varphi_s}{\partial \xi}}(0, \xi^*)(\xi - \xi*)\right) \tag{15}$$

with $\widehat{\frac{\partial \varphi_s}{\partial g}}(0, \xi^*)$ and $\widehat{\frac{\partial \varphi_s}{\partial \xi}}(0, \xi^*)$ some approximations of $\frac{\partial \varphi_s}{\partial g}(0, \xi^*)$ and $\frac{\partial \varphi_s}{\partial \xi}(0, \xi^*)$. When the situation g_{ms} of the sensor w.r.t. the platform is known, and a model of φ is available, Eq. (14) can be used to derive model-based estimates.

However, it is often difficult in practice to have a very accurate model of φ. Furthermore, what is in fact needed for the calculation of g is φ^{-1}, the inverse of φ. Having an analytical expression of φ does not imply that an analytical expression of φ^{-1} is available. When it is not, one can compute an estimate of $\varphi^{-1}(s)$ via a gradient search algorithm based on the use of the Jacobian matrix $\frac{\partial \varphi}{\partial g}$. Another possibility consists in determining a function $\hat{\varphi}$ which approximates φ in some domain containing the desired situation $g^*_{ts} = \varphi^{-1}(s^*)$, and the inverse of which has an analytical expression. This yields the estimate $\hat{g} = g_{rt}\hat{\varphi}^{-1}(s)g_{sp}$. Finally, even when an analytical expression of φ^{-1} is known, one may use a simplified expression for this function, in order to reduce the calculation load. This yields an estimate of g of the form $\hat{g} = g_{rt}\widehat{\varphi^{-1}}(s)g_{sp}$.

B. Sufficient conditions for ultimate boundedness and convergence

Now, let $\hat{z} := \hat{g}f(\alpha)^{-1}$. Assuming that the reference velocity c_r is unknown (in the contrary case, feedforward control can of course be used to improve the tracking precision) and using $\hat{z}$ instead of z in the feedback law (12)-(13) yields the following control:

$$\bar{v} = \bar{C}(\alpha)^{\dagger}\mathrm{Ad}^X(f(\alpha)^{-1})X(\hat{z})^{-1}K\hat{z} \tag{16}$$

The question is now to determine the properties of this control in terms of stability and convergence. To this purpose, we assume that $\hat{g}$ depends only on g, i.e. $\hat{g} = \psi(g)$. This is a natural assumption when the sensor is rigidly attached to the platform (i.e. $\xi \equiv \xi^*$), since s only depends on g in this case. The extension to the case where ξ is actively controlled will be discussed and illustrated through application examples in the subsequent sections. Beside the requirement of $\hat{g}$ being a function of g, the following assumption is also made.

Assumption IV.1 *There exist some constants $\delta_1 > 0$ and $\gamma_1 < 1$ such that the estimation error $\tilde{g} = g\hat{g}^{-1}$ satisfies the inequality*

$$\|\tilde{g}\| \leqslant \gamma_1\|g\|\,, \quad \forall g \in \mathrm{B_g}(\delta_1) \tag{17}$$

Condition (17) means that the relative norm of the estimation error is less than one in some bounded domain containing $g = 0$. This is clearly a weak requirement. Indeed, since $\hat{g} = \psi(g)$ then, provided that $\psi(0) = 0$ (unbiased estimation at the desired location), one shows from the group law (1) that

$$\tilde{g} \approx \left(I_3 - \frac{\partial \psi}{\partial g}(0)\right)g \tag{18}$$

in the neighborhood of $g = 0$. Therefore, if $\|I_3 - \frac{\partial \psi}{\partial g}(0)\| < 1$, Assumption IV.1 is satisfied in some neighborhood of $g = 0$. For example, when $\hat{g}$ is defined according to (15) (with $\xi \equiv \xi^*$), this relation becomes

$$\left\| I_3 - \left(\widehat{\frac{\partial \varphi_s}{\partial g}}(0)\right)^{-1}\frac{\partial \varphi_s}{\partial g}(0)\right\| < 1$$

This latter relation is reminiscent of a classical requirement upon the interaction matrix made in the context of sensor-based control of manipulator arms.

The following result establishes the ultimate boundedness of the tracking error g (compare with Property *iii.a)* in Proposition III.1).

Proposition IV.1 *Consider the feedback law* (16) *with $K = -kI_3$ $(k > 0)$ and f a transverse function. If*

$$\|g(0)\| < \delta_1 - 2\varepsilon_f \quad \text{and} \quad \bar{\varepsilon}_f := \frac{\varepsilon_f + \|c_r\|_{\max}/k}{1-\gamma_1} < \delta_1 \tag{19}$$

with δ_1 and γ_1 some constants specified by (17) *and $\|c_r\|_{\max} := \max_t \|c_r(t)\|$, then $\|g\|$ is ultimately bounded by $\bar{\varepsilon}_f$.*

Let us make some comments on this result. First, the choice of the gain matrix K in the proposition is essentially made in order to simplify the proof and specify an ultimate bound for $\|g\|$. The ultimate boundedness is also guaranteed for other Hurwitz stable matrices, like e.g. any matrix of the form

$$K = \begin{pmatrix} -K_p & 0 \\ 0 & -k_\theta \end{pmatrix}$$

with K_p a 2×2 definite positive matrix and $k_\theta > 0$. Then, Condition (19) indicates how the "size" of the transverse function f influences the ultimate bound of g and the set of initial conditions $g(0)$ for which the boundedness can be proven. Finally, let us insist on the contribution of the present result: it points out that for *any* estimation $\hat{g}$ of g satisfying (17), the tracking error with respect to *any* reference trajectory is ultimately bounded by a value that can be made arbitrarily small by a proper choice of the control parameters ε and k.

We now address the issue of convergence to a fixed situation when the target is motionless (compare with Property *iii.b)* in Proposition III.1).

Proposition IV.2 *Consider the feedback law* (16) *with $K = -kI_3$ $(k > 0)$, and f a transverse function defined by* (10)*. Let γ_2 denote the smallest constant such that*

$$\|\frac{\partial \psi}{\partial g}(g) - \frac{\partial \psi}{\partial g}(0)\| \leqslant \gamma_2\|g\|\,, \quad \forall g \in \mathrm{B_g}(\varepsilon_f/(1-\gamma_1)) \tag{20}$$

There exist two positive numbers c_1 and c_2 such that if i) $c_r = 0$, ii) (19) *is satisfied, and iii)*

$$\bar{\gamma} := \left(\gamma_1 + (\gamma_1+\gamma_2)\frac{\varepsilon_f}{1-\gamma_1}\right)\left(\frac{c_1}{\varepsilon_f} + c_2\varepsilon_f^3\right) < 1 \tag{21}$$

then $\hat{z}$ exponentially converges to zero and g exponentially converges to a fixed value.

With respect to Proposition IV.1, the above result involves the additional condition (21). For $\varepsilon_f \in [0, \bar{\varepsilon}]$, condition (21) is satisfied if

$$\left(\gamma_1 + (\gamma_1+\gamma_2)\frac{\varepsilon_f}{1-\gamma_1}\right)\frac{\bar{c}_1}{\varepsilon_f} < 1 \tag{22}$$

with $\bar{c}_1 = c_1 + c_2\bar{\varepsilon}^4$. It is clear that this condition cannot be satisfied, when ε_f tends to zero, unless $\gamma_1 = 0$. This suggests that very small values of ε_f, yielding very precise tracking, may not allow the robot to converge to a resting situation when the target is motionless. This is consistent with the difficulty of achieving both exponential stability of a fixed situation and robustness of this property w.r.t. modeling errors in the case of nonholonomic vehicles (see [7] for more details). Nevertheless, the condition (21) shows also that, for any value of ε_f, exponential convergence occurs if γ_1 and γ_2 are small enough. It follows from (18) that γ_1 is small in the neighborhood of $g = 0$ if the Jacobian of ψ at this point is close to the identity. For example, when $\hat{g}$ is given by (15), this condition is satisfied if the Jacobian of the function φ_s is accurately estimated. In this case, if one assumes, to simplify, that $\gamma_1 = 0$, then condition (22) simplifies to $\gamma_2\bar{c}_1 < 1$. The constant $\bar{c}_1$ can be calculated from the parameters of the transverse function. As for γ_2, it is directly related to second order terms of the function ψ and, thus, to second order terms of the signal function φ_s. For this reason, unless an analytic model of φ_s is known, it is usually difficult to evaluate γ_2. Let us note, however, that $\gamma_2 = 0$ when ψ is a linear mapping. Finally, let us remark that (21) is only a *sufficient* condition for convergence. Simulation and experimental results, like those presented in the next sections, tend to indicate that it is quite conservative. In fact, extensive simulations with various choices of the signal function did not allow us to observe situations for which the tracking error remained bounded but did not converge to a fixed value. Whether this property is, or is not, always satisfied thus remains an open question.

V. SIMULATION RESULTS FOR A VISION-BASED SENSOR

The simulation results presented below have been obtained with the system depicted on Fig. 2, composed of a unicycle-like robot equipped with a pan video camera. The target is materialized by three noncollinear points, labelled as L, M, and R, which are the vertices of an isosceles triangle of base $2a$ and height b, with $a = b = 0.25$. The sensor signal is $s = (\mathbf{l}, \mathbf{m}, \mathbf{r})'$, with $\mathbf{l}, \mathbf{m}, \mathbf{r}$ denoting the x-coordinates (in the camera frame) of the projection of the points L, M, R on the image plane. For all simulations, $g_{tr} = (-2.5, 0, 0)'$ (this corresponds to the platform being aligned with the target at the reference situation, as shown on the figure), and $g_{ps} = (0.51, 0, \xi)'$.

Due to space limitations, we only illustrate the use of the model-free pose estimate defined by (15). This model requires to estimate the Jacobian matrices $\frac{\partial \varphi_s}{\partial g}(0, \xi^*)$ and $\frac{\partial \varphi_s}{\partial \xi}(0, \xi^*)$. This can be done by generating small displacements $\Delta g(p), \Delta\xi(p)$ $(p = 1, \dots, P)$ in the neighborhood of $g = 0$ and $\xi = \xi^*$, measuring the associated signals' variations $\Delta s(p)$, and setting for instance (among other possibilities) $(\widehat{\frac{\partial \varphi_s}{\partial g}}(0, \xi^*)\ \widehat{\frac{\partial \varphi_s}{\partial \xi}}(0, \xi^*)) = \Delta s\, \Delta(g, \xi)^\dagger$ with

$$\Delta s = (\Delta s(1) \cdots \Delta s(P)),\ \Delta(g, \xi) = \begin{pmatrix} \Delta g(1) \cdots \Delta g(P) \\ \Delta\xi(1) \cdots \Delta\xi(P) \end{pmatrix}$$

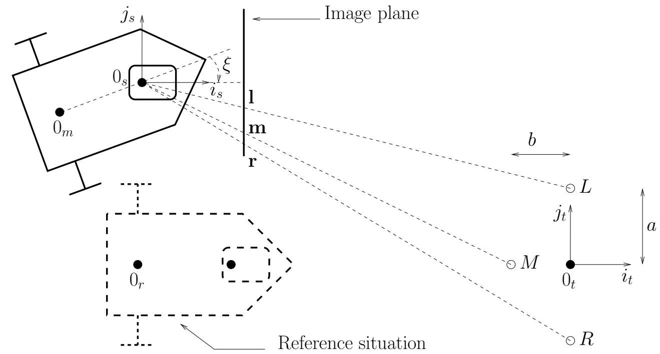

Fig. 2. Unicycle-like robot with a vision-based sensor

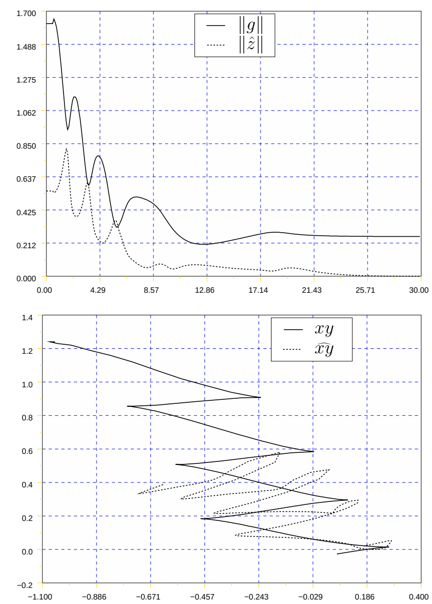

Fig. 3. Model-free estimation of g, no pan-control of the camera, fixed target

A. Fixed camera pan angle

We first consider the case when $\xi = \xi^* = 0$. Then both s and $\hat{g}$ depend on g solely, so that the analysis of Section IV-B applies. The simulation results reported on Fig. 3 have been obtained with a fixed target. The norms of g and $\hat{z}$ are displayed on the top sub-figure, and the bottom sub-figure corresponds to the motion of the origin 0_m of the robot's frame in the plane. The actual motion is shown in plain lines whereas the motion deduced from the pose estimate (15) is shown in dashed lines. The control law (16) has been applied with $K = -0.5I_3$, and with the transverse function defined by (10) for $\varepsilon = 0.3$ and $\eta = 1$. Despite the poor quality of the estimation of g when the robot is far from the desired location, the controlled variable $\hat{z}$ converges to zero and the platform converges to a fixed situation near the desired one.

B. Active control of the camera pan angle

In practice, it is often necessary to control the pan angle ξ so that the target remains inside the field of view of the camera.

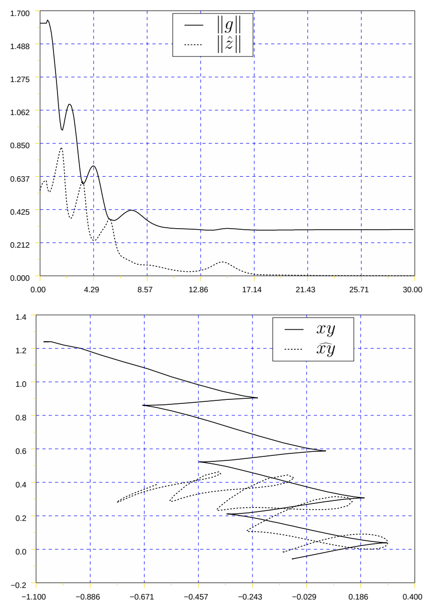

Fig. 4. Model-free estimation of g, pan-control of the camera, fixed target

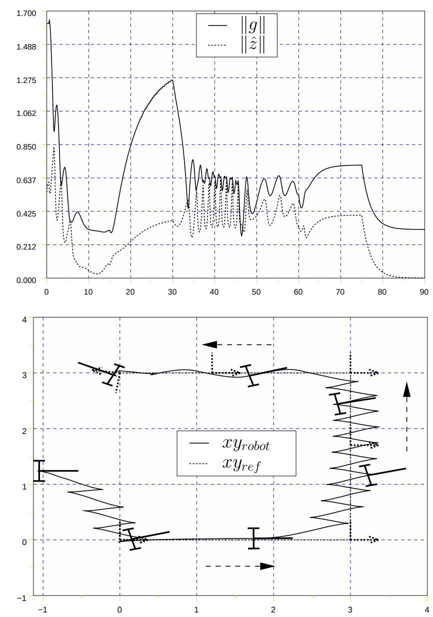

Fig. 5. Model-free estimation of g, pan-control of the camera, moving target

A simple control strategy consists in choosing v_ξ $(= \dot{\xi})$ in order to stabilize $\mathbf{m} = s_2$ to the desired value $s_2^* = 0$ (see Fig. 2). To this purpose, the following control for the camera:

$$v_\xi = k_s(s_2 - s_2^*) - v_2 \quad (k_s > 0) \tag{23}$$

can be used. Fig. 4 illustrates this strategy. The control law (16) has been applied with the same gain matrix K and transverse function as in the previous simulation, and with the control v_ξ defined by (23) for $k_s = 3$ and s expressed in metric coordinates. While the estimation of the platform's situation is significantly different from the one obtained for the previous simulation, the actual platform's motion is not much different qualitatively.

The same control strategy is illustrated on Fig. 5 in the case of a moving target. The reference velocity c_r is defined as follows:

$$c_r(t) = \begin{cases} (0,0,0)' & \forall t \in [0,15) \bigcup [75,90] \\ (0.2,0,0)' & \forall t \in [15,30) \\ (0,0.2,0)' & \forall t \in [30,45) \\ (-0.2,0,0)' & \forall t \in [45,60) \\ (0,0,0.2)' & \forall t \in [60,75) \end{cases}$$

The motions of the robot (plain lines) and reference frame (dashed lines) are shown on the lower sub-figure. One can observe that the robot executes many manœuvres for $t \in [30,45)$. This is related to the fact that the reference trajectory is not feasible on this time-interval since $c_{r,2} \neq 0$. While the tracking is correctly performed, the tracking error increases when $c_r(t) \neq 0$ (as shown on the upper sub-figure). The use of feedforward control, when c_r is known or can be accurately measured/estimated, improves this point significantly.

VI. Experimental results

We now present experimental results obtained with ANIS: a unicycle type mobile platform carrying a 6-DOF manipulator arm with a video camera mounted at its extremity. More details on the robot's architecture can be found on [13]. The robotic setup is the same as the one described by Fig. 2 and the geometric parameters which specify the tracking task are also those considered in the simulations, i.e. $g_{tr} = (2.5,0,0)'$, $g_{ms} = (0.51,0,\xi)'$, and $a = b = 0.25$. Since we do not have sensors measuring the target's situation w.r.t. an inertial frame, only experiments with a fixed target are reported here.

The model-free estimation $\hat{g}$ given by (15) is used in the control law, with the Jacobian matrices $(\frac{\partial \varphi_s}{\partial g}, \frac{\partial \varphi_s}{\partial \xi})$ being estimated via the procedure described in Section V, with the displacements $\Delta g(p)$ measured by odometry. The components of the signal vector s are given in pixels. The control law for the unicycle is given by (16) with $K = -0.5 I_3$, and f defined by (10) with $\eta = 1$ and $\varepsilon = 0.3$. The control for the camera pan angle is given by (23) with $1/k_s = -\widehat{\frac{\partial \varphi_{s,2}}{\partial \xi}}(0,0)$. In these experiments, a low-pass filter has been applied to the visual data in order to reduce the measurement noise. The motion of the robot in the cartesian plane is shown on Fig. 6 (bottom). The "pseudo-true" data corresponds to a geometric reconstruction of g based on the camera's intrinsic parameters and target's geometry. This data, purposefully not used in the control law in order to test its robustness w.r.t. large pose estimation errors, provides a more accurate estimation of the actual robot's displacement.

References

[1] Y. Shirai and H. Inoue, "Guiding a robot by visual feedback in assembling tasks," *Pattern Recognition*, vol. 5, pp. 99–108, 1973.

[2] C. Samson, M. Leborgne, and B. Espiau, *Robot Control: The Task-function Approach*, ser. Oxford Engineering. Oxford University Press, 1991, no. 22.

[3] B. Espiau, F. Chaumette, and P. Rives, "A new approach to visual servoing in robotics," *IEEE Trans. on Robotics and Automation*, vol. 8, pp. 313–326, 1992.

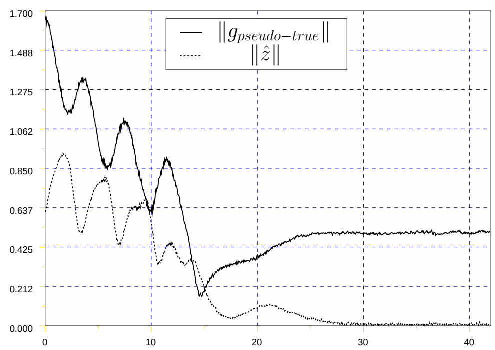

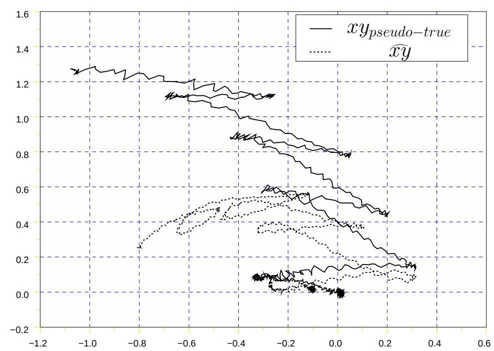

Fig. 6. Experimental results

[4] S. Hutchinson, G. Hager, and P. Corke, "A tutorial on visual servo control," *IEEE Trans. on Robotics and Automation*, vol. 12, pp. 651–669, 1996.

[5] R. Pissard-Gibollet and P. Rives, "Aplying visual servoing techniques to control a mobile hand-eye system," in *IEEE Conf. on Robotics and Automation (ICRA)*, 1995, pp. 166–171.

[6] A. Das, R. Fierro, V. Kumar, B. Southall, J. Spletzer, and C. Taylor, "Real-time vision-based control of a nonholonomic mobile robot," in *IEEE Conf. on Robotics and Automation (ICRA)*, 2001.

[7] P. Morin and C. Samson, "Trajectory tracking for non-holonomic vehicles: overview and case study," in *4th Inter. Workshop on Robot Motion Control (RoMoCo)*, K. Kozlowski, Ed., 2004, pp. 139–153.

[8] D. Lizárraga, "Obstructions to the existence of universal stabilizers for smooth control systems," *Mathematics of Control, Signals, and Systems*, vol. 16, pp. 255–277, 2004.

[9] R. Brockett, "Asymptotic stability and feedback stabilization," in *Differential Geometric Control Theory*, R. Brockett, R. Millman, and H. Sussmann, Eds. Birkauser, 1983.

[10] P. Morin and C. Samson, "Practical stabilization of driftless systems on Lie groups: the transverse function approach," *IEEE Trans. on Automatic Control*, vol. 48, pp. 1496–1508, 2003.

[11] G. Artus, P. Morin, and C. Samson, "Tracking of an omnidirectional target with a nonholonomic mobile robot," in *IEEE Conf. on Advanced Robotics (ICAR)*, 2003, pp. 1468–1473.

[12] ——, "Control of a maneuvering mobile robot by transverse functions," in *Symp. on Advances in Robot Kinematics (ARK)*, 2004, pp. 459–468.

[13] D. Tsakiris, K. Kapellos, C. Samson, P. Rives, and J.-J. Borelly, "Experiments in real-time vision-based point stabilization of a nonholonomic mobile manipulator," in *Experimental Robotics V: The Fifth Int. Symp.*, A. Casals and A. de Almeida, Eds. Springer-Verlag, 1998.